Corrosion behavior of nickel and cobalt coatings obtained by high-velocity oxy-fuel (HVOF) thermal spraying on API 5CT P110 steel

C. S. Brandolt*, M. R. Ortega Vega, T. L. Menezes, R. M. Schroeder and C. F. Malfatti

The API 5CT P110 steel is employed in oil and gas industry due to its excellent mechanical properties. However, its poor corrosion resistance makes necessary the employment of a protection. Although nickel-based and cobalt-based coatings obtained by HVOF have been widely studied regarding corrosion resistance, they are normally associated with other elements. Pure nickel and/or pure cobalt HVOF-obtained coatings have not yet been studied. Therefore, in this work, the corrosion resistance of nickel and cobalt coatings obtained by high-velocity oxy-fuel thermal spraying on API 5CT P110 steel was evaluated. The coatings were characterized regarding morphology and structure by SEM, EDS, XRD, roughness, and Vickers microhardness. The corrosion resistance was evaluated by OCP monitoring and potentiodynamic polarization in a 3.5 wt% sodium chloride solution. The results showed that both coatings acted as a barrier and avoided the contact between the steel substrate and the electrolyte due to the low melting point of the metals employed, which resulted in effective fusion of the particles. Besides, the nickel coating, promoted a better corrosion resistance compared to cobalt coating.

1 Introduction

With the increase of energy demand in recent years, the need for oil exploration in remote and critical areas, such as in deep and extremely deep waters arose. In these environments materials are subjected to high pressures and come into contact with aggressive species, hence there is a need for new technologies and materials able to withstand these extreme conditions. API 5CT P110 is a high strength low alloy (HSLA) steel, used for oil well drilling, whose specifications are described in the standard API specification 5CT-specification for casing and tubing [1]. Despite being one of the most important series of steels for pipes, API steels show corrosion resistance for short time [2]. The application of coatings on pipes of the P110 series is an effective alternative to improve the corrosion resistance of this material, which was shown by *Lin* et al. [3].

Among the options for protecting components in the oil and gas industry, the thermal spraying has received prominence as an alternative for the sector and motivated research [4–7]. Thermal spraying consists of a set of techniques for obtaining coatings whose primary purpose is to confer wear and corrosion resistance of components. In this technique, materials in powder form are heated in the beak of a pistol and accelerated by gases under pressure against the surface to be coated, reaching it in the molten state or half molten state. When hitting with the surface, the particles flatten and cling to the base material resulting in a lamellar structure consisting of flattened particles parallel to the substrate surface, containing oxides inclusions, voids, and porosity [8,9].

The thermal spraying stands out for its practicality, for its relatively low cost compared to other processes, the possibility of obtaining ceramic, metal, composites, and even polymeric coatings, in the various different substrates [8,10]. Moreover, when compared to other processes, it implies less environmental impact combined with lower cost and higher production rate. In addition to providing corrosion and wear resistance, coatings are also applied in pieces that require thermal insulation [11], electrical insulation, and biological compatibility [12]. Also, this type of coating is used to protect pipes from the oil and gas industry against erosion. Other studies show coatings by thermal spraying as an option for corrosion protection in high temperature boiler pipes [13,14]. Moreover, the use of thermal spraying coating against corrosion of magnesium alloys for aerospace applications is analyzed by *Taltavull* et al. [15]. Recently, the study of nanostructured coatings have strengthened, as at *Kumar* et al. [16] study, related to nanostructured thermal spray coating for erosion–corrosion protection of boilers.

C. S. Brandolt, M. R. Ortega Vega, T. L. Menezes, R. M. Schroeder, C. F. Malfatti
LAPEC, Federal University of Rio Grande do Sul – UFRGS, Avenida Bento Gonçalves, 9500 Porto Alegre – RS (Brazil)
E-mail: cristiane.brandolt@ufrgs.br

The thermal spraying is broken down into several processes with regard to the material to be applied, the heating method and the method of particle acceleration toward the substrate [17,18]. Among the techniques, the high-velocity oxy-fuel (HVOF) thermal spraying stands out for being operational at lower temperatures and for the highest quality of the obtained coating. In this process, there is a reaction between a fuel, introduced in a combustion chamber, and oxygen. Combustion is initiated by an ignition system and the energy released in the reaction is converted into heat and pressure to heat and propel powder particles along with the gases, forming a jet of flame. The particles in the jet reach hypersonic speed, forming a coating with extremely low porosity (typically <1%) and high strength of adhesion to the substrate [19–23].

Among the materials for thermal spraying application, nickel and cobalt are the dominant ones for presenting good corrosion resistance in various corrosive medium. These metals are widely used as base metal in super alloys or special alloys for improving corrosion and high temperature oxidation behavior [24–26].

Additionally, those metals have relatively low melting temperatures compared to the operating temperatures of the HVOF process, which guarantees a better fusion of particles, important aspect for the final quality of the coatings [18,26]. Inefficient fusion of particles of the sprinkled coating is associated with lower coating performance for the protection of the substrate. Higher operating temperatures, regarding the fusing temperature of the metal or alloy used in coating, are indicated to ensure an efficient particle fusion and to improve the performance of coatings [27]. However, some processes present operating temperature limits.

The studies of nickel and cobalt HVOF coatings associated with other elements have been reported extensively in literature regarding corrosion resistance improvement [28–33], hot corrosion [34,35], and corrosion associated with wear and erosion phenomena [36–38], however, the study of pure nickel and pure cobalt coatings obtained by HVOF has not been studied.

Therefore, in this work, pure cobalt and pure nickel coatings were obtained by a HVOF thermal spraying method, on API 5CT P110 steel. The aim of this research is to evaluate the corrosion performance of these coatings as an alternative for protection of steel pipes in aggressive environments.

2 Materials and methods

2.1 Coating obtaining

Rectangular API 5CT P110 steel substrates with dimensions of $90 \times 14 \times 8\,\mathrm{mm}^3$ were used for this study. Prior to spraying, the samples were cleaned with acetone in ultrasound for 5 min, followed by sandblasting with alumina. The prior preparation of the surface is the stage with a highest influence for the resistance and adhesion of the coating to the substrate, since it includes the elimination of impurities that might decrease the adhesion (by cleaning in acetone) and for obtaining superficial roughness (obtained by blasting), that is the main responsible for the mechanical anchoring of the coating to the substrate [39]. In order to obtain the coatings, nickel powder (99.9425%) and cobalt powder (99.9000%) were used, and the particle size was analyzed by the CILAS 1180 equipment. The coatings were obtained by HVOF thermal spraying technique with TAFA JP 5000 HP/HVOF System Model 5120 equipment of the manufacturer PRAXAIR and a TAFA GUN Model 5220 pistol. The parameters used for both coatings are displayed in Table 1.

2.2 Morphological and structural characterization

The thickness and porosity of the nickel and cobalt coatings were obtained using the Axion Vision software. The coated surface roughness was characterized by a roughness meter (Mitutoyo SJ500 model).

The determination of present phases in the coatings and metallic powders was performed by X-ray diffraction (XRD) on a Philips X-ray analytical equipment X'Pert-MPD system equipment, PW3040/00 console and the X-ray tube was the PW3373/00 tube with a Cu anode. The hardness values were obtained by Vickers microhardness testing of the nickel and cobalt coatings, as well as from the API 5CT P110 steel substrate, and from pure nickel and pure cobalt plates. In microhardness testing, a load of 0.02 kgf with 14 s of penetration was used.

The morphology of metal powders and coatings was evaluated with the use of scanning electron microscopy (SEM), in a JEOL 5800 microscope coupled to energy dispersive spectroscopy (EDS) used for elemental mapping, both in top view as cross section view.

2.3 Electrochemical characterization

For the electrochemical characterization, potentiodynamic polarization tests and open circuit potential monitoring (OCP) were performed in a potenciostat/galvanostat AUTOLAB. A three electrode cell was used with a saturated calomel electrode (SCE) as reference electrode and platinum as counter electrode, in a naturally ventilated environment, without agitation, at room temperature, in a 3.5 wt% sodium chloride solution. The OCP values were obtained during the first hour of immersion, before the potenciodynamic polarization which was carried out from −200 to 1000 mV in relation to the OCP value, with a scan rate of 1 mV/s. From the potentiodynamic polarization curves, by Tafel

Table 1. Thermal spraying parameters used in obtaining coatings of nickel and cobalt

Feed rate	0.0013 kg/s
Canon	0.152 m
Oxygen pressure	965000 ± 3440 N/m
Oxygen flow	0.0162 m^3/s
Fuel pressure	917000 ± 3440 $\mathrm{N/m}^2$
Fuel flow	0.000547 m^3/s
Nitrogen-gas pressure drag	344000 $\mathrm{N/m}^2$
Nitrogen-gas flow of drag	0.0000787 ± 0.00000787 m^3/s
Compressed air pressure	800000 $\mathrm{N/m}^2$
Speed of disk feeder	0.092 rev/s
Distance of the pistol	0.3 m
Displacement speed gun	19 m^3/s
Number of passes	4

extrapolation Nova® software, the values of the corrosion potential (E_{corr}), the corrosion current density (i_{corr}), and the polarization resistance (Rp) were obtained.

Electrochemical tests were performed on the following systems: API 5CT P110 steel with abrasive blasting, nickel coating on API 5CT P110 steel, cobalt coating on API 5CT P110 steel, pure nickel plate (99.9% purity), pure cobalt plate (99% purity), nickel coating removed from API 5CT P110 steel, and cobalt coating removed from API 5CT P110 steel.

Pure nickel and pure cobalt plates were used in the electrochemical tests aiming to compare with the coatings performance. The nickel and cobalt coatings obtained by HVOF removed from the substrate were used to evaluate the behavior toward corrosion of the coatings without the interference of the substrate. Therefore, the nickel and cobalt coatings were obtained by HVOF on the API 5CT P110 substrate and subsequently removed. The coating detachment is possible because, generally, for thermal spraying coating there is no dilution between the coating and the substrate [8], since the material reaches the substrate in the paste form and not in the melted form.

3 Results and discussion

3.1 Morphological and structural characterization

The results for the granulometric distribution of powders, exhibited values of average diameter of 27.25 μm for the nickel powder and 32.71 μm for the cobalt powder. For application by the HVOF process, the ideal average particle size is between 45 and 5 μm [10]. On the SEM images obtained after treatment displayed in Fig. 1, it appears that both powders have irregular morphology, but with a tendency to spherical shape. This morphology is desirable for the HVOF thermal spraying process, as it allows for better drainage of the spray pistol powders for coating [40–42]. The X-ray diffractograms of nickel and cobalt powders are, respectively, shown in Fig. 2A and B. The diffractions of powders revealed just the presence of pure nickel and pure cobalt, without indication of contamination of the powders or the presence of other phases.

Table 2 shows the mean values of 10 layer thickness measurements made over the coatings of nickel and cobalt and their respective standard deviation. The layer thickness is a function of several parameters of spraying, whose combination controls the thickness of the layer. In a study where pure niobium coatings were obtained by HVOF [43], five layers of coatings were obtained at a deposition rate of 41 g/min, which resulted in a layer thickness of 100 μm. In comparison with the present study, four layers have been obtained at a deposition rate of 76 g/min and thicknesses of ~200 μm were achieved. It demonstrates that the deposition rate is a more important parameter than the number of passes. In addition, higher deposition rates result in lower application times and increase the yielding of the process. Finally, from the values of standard deviation, the cobalt coating developed more thickness irregularity than the nickel coating.

The porosity is an important parameter of the performance of coatings obtained by thermal spraying, mainly in relation to corrosion. The presence of porosities (in particular, passing porosities) and discontinuities may favor the entry of the

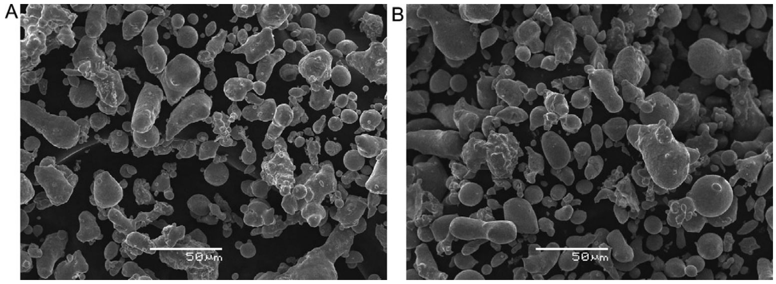

Figure 1. Images obtained by scanning electron microscopy of nickel powder (A) and cobalt powder (B)

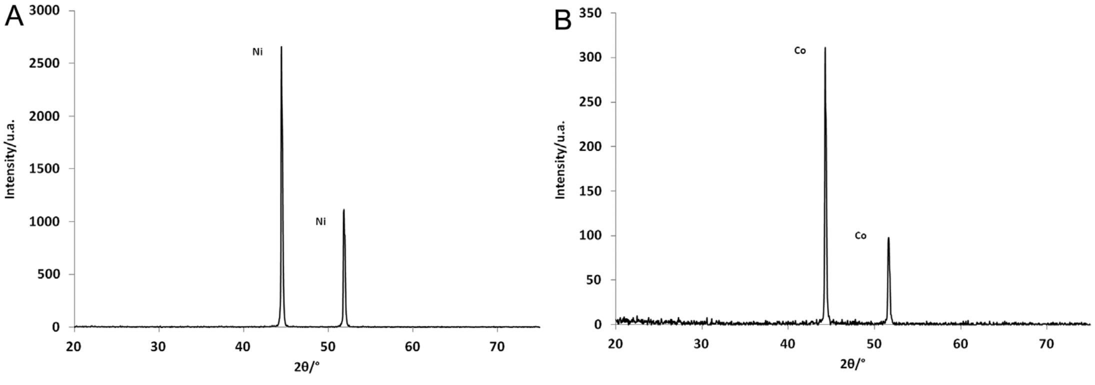

Figure 2. X-ray diffractograms of nickel powder (A) and cobalt powder (B)

Table 2. Layer thickness values obtained from the coatings of nickel and cobalt

	Nickel coating (μm)	Cobalt coating (μm)
Average thickness (μm)	202.65	208.55
Standard deviation (μm)	6.65	15.69

electrolyte and promote the chemical attack of the substrate [27]. From the results retrieved through Axion Vision software, 0.82% porosity was detected in the coating of cobalt and 0.31% porosity in the nickel coating. Both coatings showed values below 2% and are therefore within the limits set by the metallic coatings by thermal spraying N2508 standard [44]. The lowest porosity presented by nickel may be associated with the smaller size of the nickel particles in comparison with the cobalt ones. *Maranho* et al. [39] evidenced that the reduction of the particle size of the powder in the segment of 75–20 μm to the segment of 45–20 μm resulted in a decrease of porosity of 1.4–0.9%.

According to the standard N2508 [44], the reduction of the protection against corrosion in the substrate offered by the layer, occurs when there are passing porosities. However, apparently the porosity found in coatings of nickel and cobalt, as shown in Fig. 3, are not passing porosities, with only small pores that did not attach the substrate to the medium were observed. Because of the figures being two-dimensional, they do not allow the complete analysis of the pore morphology.

Table 3 displays the values of hardness (mean value of 10 measures and standard deviation) of coatings of nickel and cobalt, nickel and cobalt pure metals, and API 5CT P110 steel. It is observed that both coatings feature higher hardness values to their respective pure metals and the substrate. This result is probably associated to the formation of oxides during the thermal spraying process. Quantifications found in the literature show quantities of less than 1% of oxides formed [45]. The higher standard deviation in both coatings is probably due to the presence of irregularities and heterogeneities in the composition of coatings.

The roughness values of the nickel and cobalt coatings, and of the abrasive blasted steel are shown in Table 4. From the results, it was observed that the cobalt coating presented values of Ry, Ra, and Rms greater than the nickel coating. This variation is not very significant in terms of roughness, however, this result confirms the greater irregularity of the cobalt layer, as observed in characterization by layer thickness (Table 2).

Figure 4 displays the X-ray diffractogram of the nickel coating obtained on API 5CT P110 steel. From the results it is observed that besides the pure nickel, there was also a presence of NiO in the nickel coating. The presence of oxides in sprayed coatings is common. This is caused by the contact of the metal particles with oxygen at high temperatures during the spraying process. Thus, the formation of nickel oxide could justify the

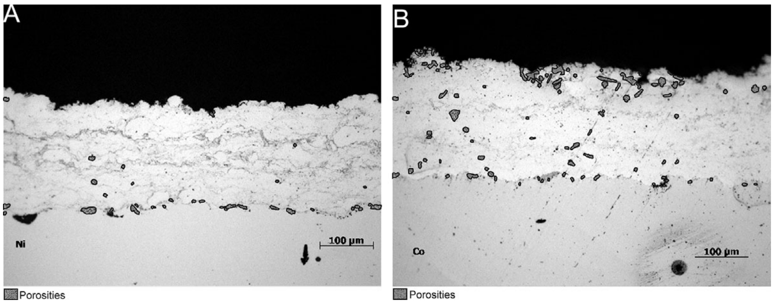

Figure 3. Zones of porosity in (A) nickel coating and (B) cobalt coating

Table 3. Values of hardness of the nickel coating, cobalt coating, pure nickel, pure cobalt, and the substrate

Measurement	Nickel coating (HV)	Cobalt coating (HV)	API 5CT P110 steel (HV)	Pure nickel plate (HV)	Pure cobalt plate (HV)
Average value	312	413	273	102	227
Standard deviation	59	70	5	4	9

Table 4. Roughness of the studied systems

System	Rms average (μm)	Rms standard deviation (μm)	Ra average (μm)	Ra standard deviation (μm)	Sy average (μm)	Sy standard deviation (μm)
Abrasive blasted API 5CT P110	6.99	0.53	5.60	0.13	45.68	2.63
Nickel coating	7.35	0.90	6.00	0.79	42.19	6.44
Cobalt coating	9.40	0.11	7.64	0.07	51.73	0.60

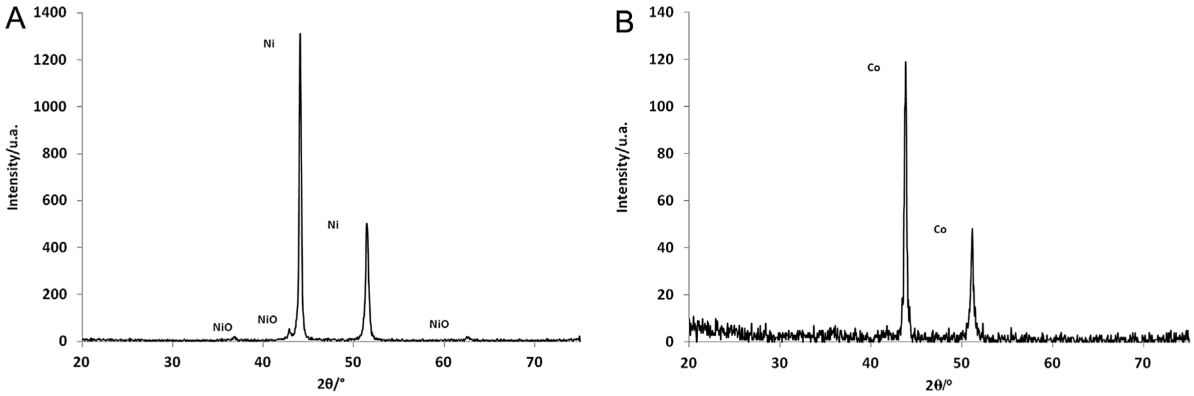

Figure 4. X-ray diffractogram of the nickel coating (A) and of the cobalt coating (B), obtained by HVOF

higher hardness value of the nickel coating in relation to the pure nickel.

On the other hand, the cobalt coating diffractogram showed only the pure metal. However, the superior hardness of the cobalt coating could indicate that there was the formation of oxides in the coating. The X-ray diffraction probably did not identify the presence of oxides due to the high roughness of the cobalt coating, associated with the lower detection intensity as the ordinate axis of the diffractogram indicates. The detection of nickel oxide in Fig. 4 was of low intensity, probably due to the roughness of the coating as well.

Figure 5 displays the top view images and Fig. 6 displays the cross-section images of the coatings of nickel and cobalt, obtained by SEM. From Fig. 5, it is noticeable that both coatings have an irregular morphology. These surface irregularities may be affected by the electrolyte by accumulating a differentiated concentration of ions, and accelerate mechanisms of localized corrosion [27].

Note that in Fig. 5 the coatings practically do not present any porosity regions along the cross-section. It is only possible to observe small microporosities along the cobalt coating, parallel to the surface, as indicated by the white arrows in Fig. 5B . Probably, this parallel distribution is due to the lamellar structure typical for thermal spraying-obtained coatings, which facilitate the occurrence of defects in the longitudinal direction of the coating. Despite of the presence of spread microporosities, no large regions of porosities or passing porosities were found. In another study [46], Nb-based coatings presented large regions of passing porosities, which, in turn, compromised their corrosion behavior.

Figure 7 shows the cross-section image of the nickel-coated steel with mappings of the Fe, and Ni elements. Figure 8 shows the cross-section image of the cobalt-coated steel with mappings

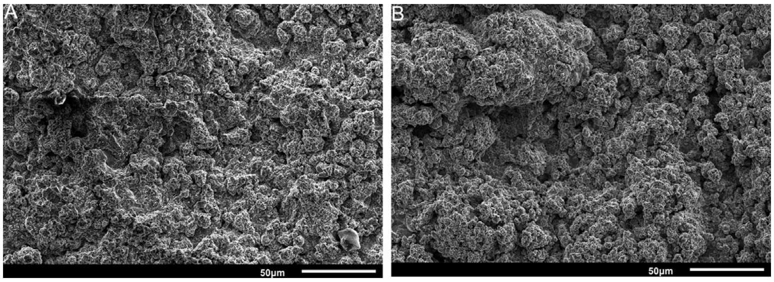

Figure 5. SEM top view images of the nickel coating (A) and the cobalt coating (B) obtained by HVOF

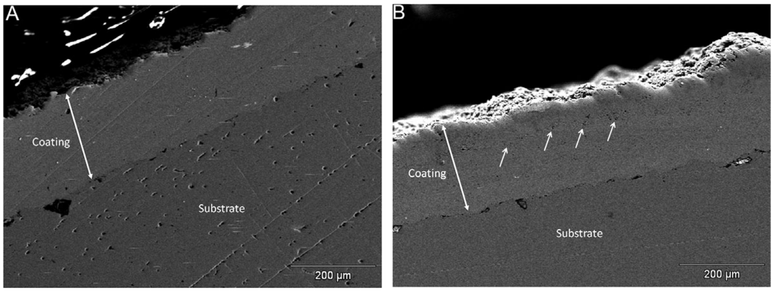

Figure 6. SEM cross-section images of the nickel coating (A) and cobalt coating (B) obtained by HVOF. In Co coating, arrows indicate porosity regions

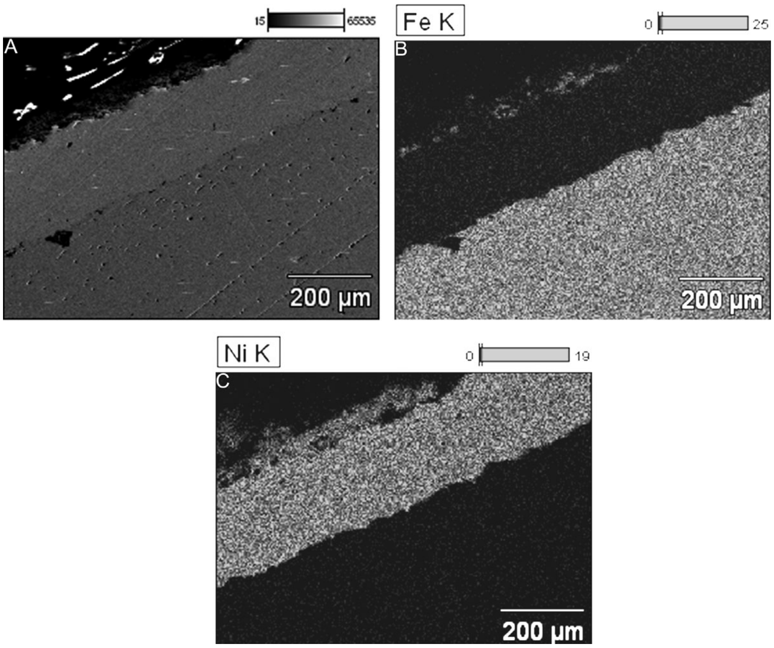

Figure 7. SEM cross-sections images of the nickel coating obtained by HVOF: (A) image obtained by secondary electrons, (B) clear region showing the mapping of element Fe, (C) clear region showing the mapping of Ni element

of the Fe and Co elements. From the pictures, it is noticeable that the composition of the coatings is homogeneous throughout its length. There was no presence of dark regions to indicate defects or presence of other elements or phases.

Figures 7 and 8 also suggest that there is also no zone of dilution between the coating and the substrate, since the separation between them is very clear. Techniques for obtaining coatings by welding have as disadvantage the existence of the dilution zone. This dilution can cause micro-structural changes in the region, which in turn may compromise the metallurgical quality of the coating. In this sense, the deposition of alloys by thermal spraying methods offer the advantage of not owning the dilution zone, since the process does not reach sufficient temperatures to melt the base metal [8].

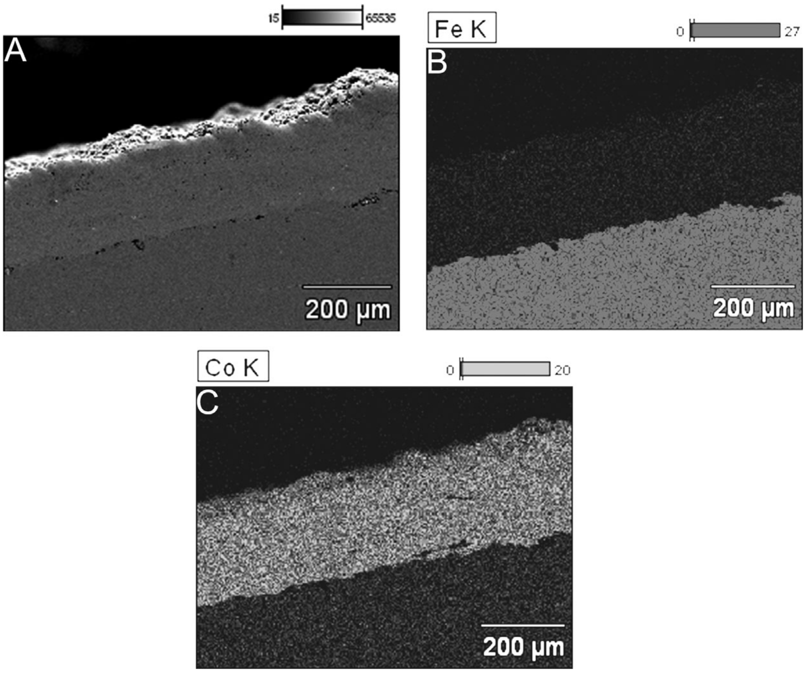

Figure 8. SEM cross-sections images of the cobalt coating obtained by HVOF: (A) image obtained by secondary electrons, (B) clear region showing the mapping of the Fe element, and (C) clear region showing the mapping of the Co element

3.2 Electrochemical characterization

3.2.1 Open circuit potential monitoring

Open circuit potential (OCP) monitoring results, during an hour of immersion before the potentiodynamic polarization test, is shown in Fig. 9. The abrasive blasted API 5CT P110 steel presented more negative potential values than the other systems during the entire period of monitoring, i.e., this system was the most active. The noblest potential values were observed for the nickel coating removed from the substrate, followed by the pure nickel plate and the nickel coating on the steel. It is noticed that the nickel coating has an excellent response to immersion in sodium chloride, both when evaluated on the steel as when evaluated removed from the API 5CT P110 steel. The observed oscillation in the nickel curve is probably due to successive depassivations and passivations in the material of the coating.

OCP curves of the cobalt coating on the steel and removed from the steel showed intermediate behavior between the curves of the nickel and of the abrasive blasted steel. This behavior evidenced that nickel coating presented better barrier effect compared to cobalt coating on the API 5CT P110 steel. This must be due to the better corrosion behavior of the metal nickel in comparison to the metal cobalt. Generally speaking, the coatings had a barrier effect and isolated the substrate from contact with the electrolyte. It demonstrates that the porosities presented by the coatings (Figs. 3 and 5) are not passing porosities, since OCP results allow to infer that the electrolyte does not reach the substrate.

3.2.2 Potentiodynamic polarization

The curves of the potentiodynamic polarization for the studied systems are shown in Fig. 10. Table 5 shows the values of the corrosion potential (E_{corr}), the corrosion current density (i_{corr}), and the polarization resistance (Rp), obtained from the Tafel extrapolation. Results show that the abrasive blasted API 5CT P110 presented the highest values of i_{corr} and the smallest values of Rp. Moreover, these systems presented more active values of potential among all the studied systems. These results maintain the trend as presented by the OCP curves in Fig. 9.

The cobalt coatings showed higher nobler values of corrosion potential polarization resistance than the abrasive blasted steel, being similar to the values of the curve of pure cobalt plate, which show the barrier effect of the cobalt coating. However, the values of i_{corr} presented by the cobalt coating are approximately the same as the ones presented by the abrasive blasted steel, which demonstrates that, in the context of the corrosion current density, it has not improved the behavior of the base material.

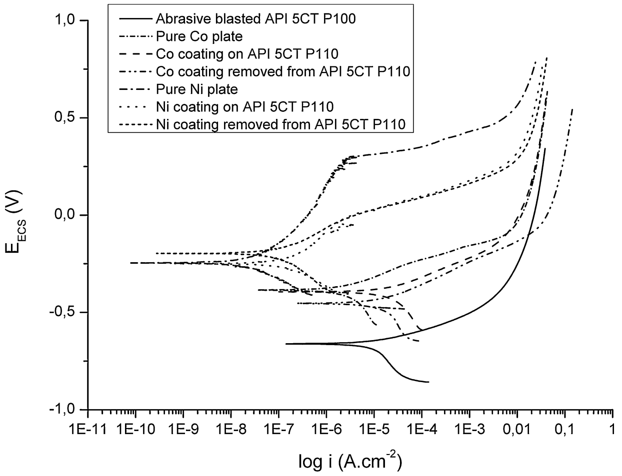

Figure 10. Potentiodynamic polarization curves for the studied systems

The nickel coatings showed improvements in the corrosion behavior of the substrate, showing values of Rp and i_{corr} similar to those of pure nickel plate. As indicated in Table 5, nickel coatings presented i_{corr} values about 100 times lower than the values of abrasive blasted steel and Rp values around 100 times higher than values of the abrasive blasted steel, which shows that the obtained nickel coating by thermal spray is an excellent choice of coating against corrosion for API 5CT P110 steel.

The highest corrosion resistance of nickel-coated API 5CT P110 steel is probably related to the choice of powders with the appropriate characteristics, especially low melting point in relation to the operating temperature of the HVOF process. It led to the production of a coating with low presence of defects, mainly the absence of passing porosity, reason why the coating acted as barrier against the electrolyte. In other researches, the porosity also had its repercussions on the electrochemical performance of the coatings. In the article of *Bezerra* [47], in which the application of a NiCr alloy is performed by thermal spraying, the low levels of porosity raised the values of polarization resistance of the coatings, in comparison to the

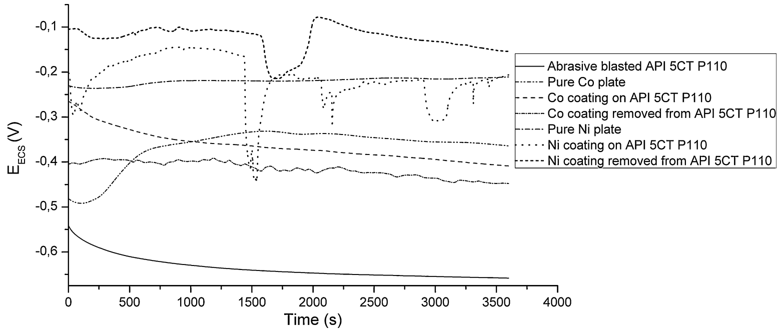

Figure 9. Open circuit potential curves for the studied systems

Table 5. Data obtained from extrapolation by the Tafel lines in experimental polarization curves of the studied systems

System	E_{corr} (mV)	i_{corr} (A/cm^2)	Rp (Ω/cm^2)
Abrasive blasted API 5CT P110	−0.659	2.15×10^{-5}	2.13×10^{3}
Pure cobalt plate	−0.382	5.50×10^{-6}	1.09×10^{4}
Cobalt coating on API 5CT P110	−0.404	2.50×10^{-5}	1.88×10^{3}
Cobalt coating removed from API 5CT P110	−0.480	4.50×10^{-5}	6.50×10^{3}
Pure nickel plate	−0.248	5.50×10^{-8}	1.20×10^{6}
Nickel coating on API 5CT P110	−0.249	3.40×10^{-7}	1.85×10^{5}
Nickel coating removed from API 5CT P110	−0.196	3.80×10^{-7}	2.78×10^{5}

substrate. On the other hand, in other work [46] which obtained coatings of niobium and niobium-iron by HVOF, large regions of porosity were found through the SEM images, in the coatings. This porosity influenced the corrosion performance, since the coatings had a much lower performance related to the pure metal (niobium) and showed similar *Rp* and i_{corr} values to the substrate.

Comparing the melting point of niobium, 2469 °C [48]; with the melting point of nickel, 1455 °C [49]; and of cobalt, 1495 °C [48], it is observed that the melting temperatures of nickel and cobalt are substantially inferior to that of niobium. This was probably the cause of the better performance of coatings obtained in this research, since powder particles probably had a melting or softening to a larger extent than in *Junior's* research. These higher softening or incipient fusions likely led to a larger plastic union at the moment of the coatings formation, as well as it must have contributed to a higher adhesion to the substrate, resulting in coatings with higher compaction and with better metallurgical structure. In the research of *Zhao* et al. [27], the inefficient fusion of particles is also associated with the lower efficiency of the coating as a barrier for the electrolyte. However, *Zhao* et al. [27] indicates higher temperatures in the process of spraying, an equally effective way for the fusion of particles. *Wang* et al. [50] also associates the inefficient fusion of particles as one of the factors that reduce corrosion resistance of HVOF coatings.

In *Motta's* research [5], niobium coatings were obtained on API 5L X65 steel by thermal plasma spraying process by varying the operation parameters electric current and number of passes. In this research, the corrosion performance of the coatings was also much lower than the performance of pure niobium metal, with the best results of corrosion current density being about 100 times higher than that of pure metal. The worst results were about 1000 times higher than the pure niobium results, not showing improvement in behavior against corrosion in relation to the API 5L X65 steel substrate. In *Motta's* research [5], beyond the high melting point of niobium, there was another reason for the bad corrosion performance of the coatings in the choice for the plasma thermal spraying process. In the plasma process, the particles reach speeds well below the speeds of the HVOF process, which in turn results in coatings with more regions of porosity and, thus, compromises their barrier effects. In other researches, the superiority of the HVOF process, concerning corrosion resistance, remained evident when compared to the plasma process, considering the smaller number of defects presented in the coating obtained by the HVOF technique [51].

Despite the demonstrations of significant improvement related to the substrate, the coatings did not show the same behavior as that of the pure metals. For example, the coatings of nickel did not show an equally efficient passivation and, therefore, did not provide current density values as low as the pure nickel plate. This small decrease of the nickel coating performance, compared to the pure nickel, which was also presented in the cobalt coating, can be associated with the presence of irregularities in the coating, as well as the presence of oxides, characteristic of the process.

The execution of the polarization tests with coatings removed from steel aimed to eliminate the interference of the substrate in the electrochemical results, in order to ensure the actual performance of the coating. From the results of the polarization, both the nickel coating removed from substrate as the cobalt coating removed from substrate showed worse corrosion behaviour compared with the respective pure metals. This confirms that the coatings obtained by thermal spraying feature a loss in corrosion performance. This can be explained by the following aspects:

- The sample surface irregularity, as revealed in the SEM images (Fig. 5) and by the roughness values (Table 4), as well as the presence of superficial cavities, capable of accumulating electrolytes, can accelerate mechanisms of localized corrosion. The pitting corrosion mechanism in passive materials in medium containing chloride ions occurs from the breakup of the passive layer and the further growth of the pits into the sample. This growth occurs from the dissolution of the metal cation inside the cavity, which reacts with water to form metal hydroxides and release hydrogen ions. The concentration of this ion results in the reduction of pH to around 1.5 inside the cavity, which contributes to the continuous propagation of the pits. Thus, the surface irregularities of sprayed layers could act as pre-formed pitting, contributing to the dissolution of the metal in the interior of cavities and irregularities. As *Zhao* et al. [27] cited, the highest coating corrosion rate is associated with the accumulation of hydrogen ions and chloride ions inside the pores, a fact that justifies the amount of corrosion products near these defects.
- Besides the superficial pores, defects inside the coatings, such as oxides and inclusions, can act favoring corrosion through the layer. In the research by *Guo* et al. [52] corrosion behavior of coatings obtained by HVOF and HVAF was compared. HVAF coatings showed better corrosion resistance due to the lower formation of oxide, because oxide rust contours formed

between the partially melted particles in HVOF coating can become the diffusion channels for the electrolyte, and cause inner corrosion of the coatings. In another research [53], the coatings obtained by spraying may suffer some crevice corrosion phenomena, due to the presence of defects, such as oxides, that act as initiation sites for corrosion.

4 Conclusions

- On the basis of the appropriate properties of the used metal in the thermal spray process, the nickel and cobalt coatings were fairly homogeneous and with a low presence of defects, due to the optimal particle sizes of the powders as well as the parameter setting of the HVOF process.
- Both coatings showed hardness values higher than their respective pure metals, which indicates oxide formation in the coatings.
- The cobalt and nickel coatings promoted an improvement in the corrosion behavior, showing a similar behavior to those of the pure metals. This was probably due to the choice of metals with low melting points, which promoted an efficient fusion of the particles contributing for the obtaining of coatings that acted as a barrier between the substrate and the electrolyte.
- Besides, the nickel coating presented a better corrosion behavior than the cobalt coating, since it has a higher intrinsic corrosion resistance, which highlighted a promising future for its implementation in oil industry components.

Acknowledgments: The authors would like to express their gratitude for the financial support of CAPES (a Brazilian Governmental Agency for the Development of Human Resources) and CNPq (the Brazilian National Council for Scientific and Technological Development). Furthermore, the authors are grateful to RIJEZA METALURGIA for providing the thermal spray coatings.

5 References

[1] API: American Petroleum Institute, *Specification for Casing and Tubing*: ISSO 11960, Washington, **2005**.
[2] S. D. Zhu, J. F. Wei, Z. Q. Bai, G. S. Zhou, J. Miao, R. Cai, *Eng. Fail. Anal.* **2011**, *18*, 950.
[3] N. Lin, J. Guo, F. Xie, J. Zou, W. Tian, X. Yao, H. Zhang, B. Tang, *Appl. Surf. Sci.* **2014**, *311*, 330.
[4] M. M. El Rayes, H. S. Abdo, K. A. Khalil, *Int. J. Electrochem. Sci.* **2013**, *8*, 1117.
[5] F. P. Motta, *Dissertation*, UFRGS Porto Alegre, Brazil, **2011**.
[6] R. M. H. P. Rodriguez, R. S. C. Paredes, S. H. Wildo, A. Calixto, *Surf. Coat. Technol* **2007**, *202*, 172.
[7] J. M. Guilemany, J. M. Miguel, S. Armada, S. Vizcaino, F. Climent, *Mater. Charact.* **2001**, *47*, 307.
[8] J. R. Davis, *Handbook of Thermal Spray Technology*, ASM International, Materials Park, Ohio **2004**.
[9] P. W. Lee, *ASM Metals Handbook—Power Metals Technologies and Applications*, ASM Int., Materials Park, Ohio **1992**.
[10] L. Pawlowski, *The Science and Engineering of Thermal Spray Coatings*, John Wiley & Sons, New York **2008**.
[11] M. S. Morsi, S. S. El Gwad, A. Shoeib, K. F. Ahmed, *Int. J. Electrochem. Sci.* **2002**, *7*, 2811.
[12] C. C. Lima, R. Trevisan, *Aspersão térmica: fundamentos e aplicações*, Artliber, São Paulo **2002**.
[13] C. Cha, H. W. Gudenau, G. T. Bayer, *Mater. Corros.* **2002**, *53*, 195.
[14] S. C. Cha, F. P. Wölpert, *Mater. Corros.* **2002**, *53*, 886.
[15] C. Taltavull, A. J. Lopez, B. Torres, A. Atrens, J. Rams, *Mater. Corros.* **2015**, *66*, 423.
[16] M. Kumar, H Singh, N. Sing, *Mater. Corros.* **2015**, *66*, 695.
[17] P. V. Marques, *Aspersão térmica*, Infosolda and UFMG, Minas Gerais **2003**.
[18] M. L. Thorpe, *Thermal Spray: Advanced Materials and Process*, Ed. American Society for Metals, Virginia, **1993**, pp. 50–61.
[19] J. Stokes, *The Theory and Application of the HVOF (High Velocity Oxy-Fuel)*, available in: http://webpages.dcu.ie/~stokesjt/ThermalSpraying/Book/HVOFThermalSpraying.htm, access in dez/**2013**.
[20] R. C. Souza, H. J. C. Voorwald, M. O. H. Cioffi, *Surf. Coat. Technol.* **2008**, *203*, 191.
[21] G. Margineana, D. Utu, *Appl. Surf. Sci.* **2012**, *258*, 8307.
[22] J. S. P. O., *Joint Service Pollution Prevention Opportunity Handbook: High Velocity Oxy-Fuel Thermal Spray*, available in http://p2library.nfesc.navy.mil/P2_Opportunity_Handbook/1_3.html, access in jan/**2014**.
[23] J. Kawakita, S. Kuroda, T. Kodama, *Surf. Coat. Technol.* **2003**, *166*, 17.
[24] L. W. A. Ladeira, *Dissertation*, UFMG Belo Horizonte, Brazil, **2000**.
[25] I. Aziz, *Corrosion of Nickel-Base Alloys*, ASM International, Materials Park, Ohio **1992**.
[26] J. R. Davis, *ASM Metals Handbook—Properties and Selection: Nonferrous Alloys and Special-Purpose Materials*, ASM Int., Materials Park, Ohio **1992**.
[27] W. M. Zhao, Y. Wang, L. X. Dong, K. Y. Wu, J. Xue, *Surf. Coat. Technol.* **2005**, *190*, 293.
[28] G. Bolelli, L. Lusvarghi, R. Giovanardi, *Surf. Coat. Technol.* **2008**, *202*, 4793.
[29] M. Karbasi, M. R. Zamanzad Ghavidel, A. Nekahi, *Mater. Corros.* **2014**, *65*, 485.
[30] A. Lekatou, D. Zois, D. Grimanelis, *Thin Solid Films* **2008**, *516*, 5700.
[31] L. Gil, M. H. Staia, *Thin Solid Films* **2002**, *420*, 446.
[32] M. M. Verdian, K. Raeissi, M. Salehi, *Appl. Surf. Sci.* **2013**, *273*, 426.
[33] J. Saaedi, H. Arabi, T. W. Coyle, S. Mirdamadi, H. Ghorbani, *Mater. Corros.* **2011**, *62*, 823.
[34] M. Oksa, P. Auerkari, J. Salonen, T. Varis, *Fuel Process. Technol.* **2014**, *125*, 236.
[35] T. S. Sidhu, S. Prakash, R. D. Agrawal, *Surf. Coat. Technol.* **2006**, *201*, 792.
[36] G. Bolelli, V. Cannillo, L. Lusvarghi, R. Rosa, A. Valarezo, W. B. Choi, R. Dey, C. Weyant, S. Sampath, *Surf. Coat. Technol.* **2012**, *206*, 2585.
[37] V. A. D. Souza, A. Neville, *Wear* **2005**, *259*, 171.
[38] J. M. Perry, A. Neville, V. A. Wilson, T. Hodgkiess, *Surf. Coat. Technol.* **2001**, *137*, 43.
[39] O. Maranho, *Thesis*, USP São Paulo, Brazil, **2006**.

[40] Y. S. Wu, D. C. Zeng, Z. W. Liu, W. Q. Qiu, X. C. Zhong, H. Y. Yu, S. Z. Li, *Surf. Coat. Technol.* **2011**, *206*, 1102.

[41] Y. Liu, G. Q. Gou, H. Chen, L. J. Wang, M. J. Tu, J. P. Yu, *Adv. Mat. Res.* **2013**, *602*, 1710.

[42] W. Yaosha, Q. Wanqi, Y. Hongya, Z. Xichun, L. Zhongwu, Z. Dechang, L. Shangzhou, *Rare Metal Mater. Eng.* **2011**, *40*, 507.

[43] L. C. Noronha, *Dissertation*, UFRGS Porto Alegre, Brazil, **2014**.

[44] N2568, *Revestimentos Anticorrosivos Aplicados por Aspersão Térmica*, Petrobras, **2011**.

[45] M. M. K. Verdian, K. Raeissi, M. Salehi, *Appl. Surf. Sci.* **2013**, *273*, 426.

[46] C. S. Brandolt, J. G. Souza Junior, S. R. Kunst, M. R. Ortega Vega, R. M. Schroeder, C. F. Malfatti, *Mater. Res.* **2014**, *17*, 866.

[47] B. S. L. Bezerra, *Dissertation*, University of Tiradentes Aracaju, Brazil, **2007**.

[48] J. R. Davis, *ASM Metals Handbook: Alloy Phase Diagrams*, ASM Int., Materials Park, Ohio **1992**.

[49] R. C. Reed, *The Superalloys: Fundamentals and Applications*, Cambridge University Press, Cambridge, UK **2006**.

[50] Y. Wang, S. L. Jiang, Y. G. Zheng, W. Ke, W. H. Sun, X. C. Chang, W. L. Hou, J. Q. Wang, *Mater. Corros.* **2013**, *64*, 801.

[51] M. M. Verdian, K. Raeissi, M. Salehi, *Corros. Sci.* **2010**, *52*, 1052.

[52] R. Q. Guo, C. Zhang, Q. Chen, Y. Yang, N. Li, L. Liu, *Corros. Sci.* **2011**, *53*, 2351.

[53] G. Bolelli, R. Giovanardi, T. Manfredini, *Corros. Sci.* **2006**, *48*, 3375.

(Received: June 16, 2015) W8505
(Accepted: August 4, 2015)